Development of an Atmospheric General Circulation Model for Integrated Earth System Modeling on the Earth Simulator

Shingo Watanabe[1]*, Hiroaki Miura[1], Miho Sekiguchi[2], Tatsuya Nagashima[3], Kengo Sudo[4,1], Seita Emori[3,1], and Michio Kawamiya[1]

[1] *Frontier Research Center for Global Change, Japan Agency for Marine-Earth Science and Technology, 3173-25, Showamachi, Kanazawa-ku, Yokohama, 236-0001, Japan*
[2] *Department of Marine Electronics and Mechanical Engineering, Faculty of Marine Technology, Tokyo University of Marine Science and Technology, 2-1-6, Etchujima, Koto-ku, Tokyo, 135-0044, Japan*
[3] *National Institute for Environmental Studies, 16-2 Onogawa, Tsukuba, Ibaraki, 305-8506, Japan*
[4] *Department of Earth and Environmental Sciences, Graduate School for Environmental Studies, Nagoya University, Furo-cho, Chikusa-ku,Nagoya, 464-8601, Japan*

Abstract This paper introduces an atmospheric general circulation model (AGCM) that better simulates the dynamical and physical processes and is used in the framework of our integrated earth system modeling. In particular, the dynamical and physical processes in the stratosphere are greatly improved compared to the previous version of the climate model. In this study, the top of the AGCM is extended to the mesopause height, and a hybrid σ-pressure coordinate system, which is suited for the simulation of transport phenomena near the tropopause, is introduced. An improved radiative transfer scheme dramatically decreases the cold bias near the tropical tropopause and the extratropical lower stratosphere. Incorporation of the non-orographic gravity wave drag parameterization with a source function based on the results of a high-resolution AGCM simulation allows the model to reproduce a realistic general circulation in the stratosphere and mesosphere.

Keywords: Earth system, Stratosphere, General circulation, Gravity wave

1. Introduction

An integrated earth-system model has been developed at the Frontier Research Center for Global Change (FRCGC) in collaboration with the Center for Climate System Research (CCSR) of the University of Tokyo and the National Institute for Environmental Studies (NIES). The objective for the development of an earth system model was to model the variations and changes in the global environment as a whole, that is, to develop an integrated system, which includes the physical climatic processes, the biogeochemical processes, and the eco-dynamical processes [1, 2].

In order to simulate long-term changes in climate systems and atmospheric chemistry, as well as seasonal and interannual variations, an appropriate representation of the stratosphere is required [3]. This paper focuses on the following three topics that are important to properly represent the physical and chemical interaction between the troposphere and the stratosphere. The first process con-

siders the thermal structure near the tropopause, which is important for chemical reactions and water vapor dehydration processes that can change with global warming. The second process considers the dynamical transport processes, such as the stratosphere-troposphere exchange and the mean meridional circulation in the stratosphere. These factors change with global warming and affect the concentration of greenhouse gases in the troposphere [4, 5]. The third and final process is the meridional structure of the stratospheric jets that can affect the tropospheric climate through dynamical connections, for example, the downward propagation of solar effects associated with the internal variability of the polar night jet [6, 7], and the downward effects of the stratospheric ozone hole in late spring [8].

This paper describes the development of an atmospheric general circulation model (AGCM) in the integrated earth-system model, which is called the Model for Interdisciplinary Research on Climate (MIROC) -

---

* **Corresponding author**: *Shingo Watanabe, Frontier Research Center for Global Change, Japan Agency for Marine-Earth Science and Technology, 3173-25, Showamachi, Kanazawa-ku, Yokohama, 236-0001, Japan. E-mail: wnabe@jamstec.go.jp*

Kyousei Integrated Synergetic System Model of the Earth (kissme). Results of MIROC-kissme show many improvements in comparison with the coupled general circulation model MIROC-mid, which was the basis from which the MIROC-kissme was developed [1, 9, 10]. The improvements described in this paper are achieved by 1) extending the top of the model, 2) changing the vertical coordinate system, 3) improving the radiative transfer scheme, and 4) incorporating non-orographic gravity wave drag parameterization. Section 2 discusses each of these improvements in greater detail. Results of the MIROC-kissme are compared with those of MIROC-mid in Section 3. Section 4 gives concluding remarks.

2. Development of the AGCM in MIROC-kissme

The MIROC-kissme was developed based on MIROC-mid. The AGCM in MIROC-mid is a global spectral model with a T42 horizontal resolution, that is an approximately 2.8˚ grid spacing in latitude and longitude. It has 20 layers from the surface to a height of 30 km. It includes a full-set of physical parameterizations such as radiation, cumulus convection, stratiform clouds, and boundary layer. The bottom boundary of the AGCM is coupled to a physical land component model and an oceanic general circulation model. Detailed descriptions of MIROC-mid are given in [9,10].

2.1 Vertical coordinate system

In order to fully resolve the stratosphere and mesosphere, the top of the AGCM is raised from about 30 km to the mesopause height of about 80 km. The number of vertical layers is increased from 20 to 80. Fig. 1 shows the vertical coordinate systems for MIROC-kissme (L80) and MIROC-mid (L20). The new vertical coordinate system has a fine vertical resolution of about 680 m in the upper troposphere to the middle stratosphere. The fine vertical resolution is one of the conditions necessary for the spontaneous generation of the equatorial quasi-biennial oscillation (QBO) in AGCMs [11, 12, 13]. In order to prevent extra wave reflection at the top boundary, a sponge layer is added to the top level, which causes the wave motions to be greatly dampened.

The terrain-following σ vertical coordinate system used in MIROC-mid cannot accurately represent transport processes over mountainous regions. This system creates unrealistic exchanges of trace constituents across the tropopause and, thus, causes huge moisture biases in the lower stratosphere. The σ vertical coordinate system has been replaced with a hybrid σ-pressure vertical coordinate system, in which the vertical coordinate system is switched to a pure pressure coordinate system above about 350 hPa [14]. The hybrid coordinate system gives
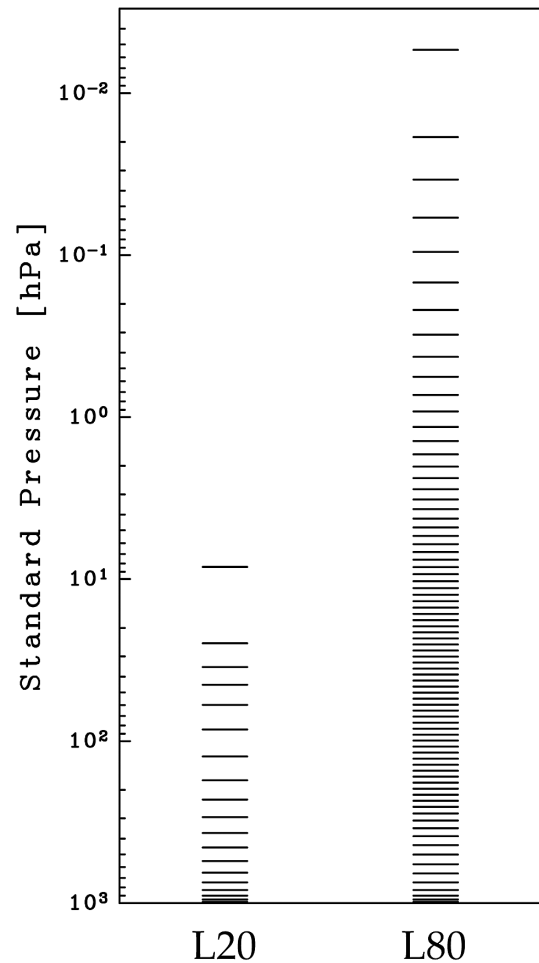

Fig. 1 Vertical coordinate system for MIROC-mid (left) and MIROC-kissme (right).

realistic results in high-resolution AGCM simulations, in terms of ozone distribution in an ozone coupled model [13], and wave dynamics associated with orographic gravity waves [15]

2.2 Radiative transfer scheme

The radiative transfer scheme used in MIROC-mid has problems with the accuracy of the heating rate calculations near the tropopause, which results in cold biases near the tropical tropopause and in the extratropical lower stratosphere [10]. In order to fix these biases, an updated version of the radiative transfer scheme is incorporated into MIROC-kissme. Major differences between these radiative schemes is that the new scheme 1) uses an updated database for line and continuum absorption, 2) considers an increased number of absorption bands, 3) reconsiders the number of integration points for the correlated-*k* distribution method, and 4) uses an improved optimization method to determine the best integration points. As a result, the accuracy of the heating rate calculation near the tropopause is greatly improved [16].

MIROC-kissme includes atmospheric chemistry in the troposphere and stratosphere [1]. The radiative transfer and photolysis of chemical constituents are consistently calculated. On the basis of the new radiative scheme, a new parameter table with 32 bands and 102 integration points, whose intervals are finer in the UV-VIS region than those used in the usual calculations and are optimized for the photolysis calculation of chemical constituents (ozone, molecular oxygen, and nitrous oxide), was developed. Using the new radiative scheme with the new parameter table allows MIROC-kissme to obtain a reasonable distribution of chemical constituents in the troposphere and stratosphere, as well as an accurate radiative heating rate.

2.3 Non-orographic gravity wave drag parameterization

Wind accelerations due to the momentum deposition of atmospheric gravity waves are important for the formation of the general circulation and thermal structure in the stratosphere and mesosphere [17]. The T42 horizontal resolution of the AGCM is insufficient to explicitly represent such gravity waves. Hence, the effects of such subgrid scale gravity waves should be considered using gravity wave drag parameterizations. The orographic gravity wave drag parameterization of McFarlane [18] is included in MIROC-mid and MIROC-kissme. In addition to the effects of the orographic gravity waves, effects of non-orographic gravity waves are important especially for driving the equatorial QBO and for the formation of the meridional structure of the mesospheric jets [17, 19].

The Doppler-Spread parameterization of Hines [20] is incorporated into MIROC-kissme. A source function of gravity waves is required by the Hines parameterization. It is a function of time, geographical location, propagation directions, and amount of vertical flux of horizontal momentum carried by the gravity waves. The tropospheric sources of the non-orographic gravity waves considered here are cumulus convection, fontal dynamics, and dynamical instability associated with jet streams. All of these are highly variable in time and geographical location. Furthermore, these sources emit different type of gravity waves, which depend not only on their own characteristics, but also on background winds and static stability [17]. Although recent estimations of the geographical distribution of gravity waves using satellites have been performed [21, 22], these data are still insufficient to determine the required complicated source function. Instead, the monthly climatology of the source function is derived from the results of the T213L256 AGCM simulation [18]. In the extratropics, an 8 azimuthal distribution for the horizontal wind variance and the vertical flux of

horizontal momentum due to gravity waves that cannot be resolved in the horizontal resolution of T42, which is a horizontal wavelength of less than about 950 km, are considered. In the source function, the quasi-stationary gravity waves are filtered out with a running average of 48 hours, because they are considered as orographic gravity waves whose effects are separately parameterized with the McFarlane scheme. The source function is derived at about 70 hPa, where dominant gravity waves are those vertically propagating, that is, the source function should not include approximately horizontally propagating inertia gravity waves. In the tropics, an isotropic source is launched at 100 hPa. This is required, because the source function derived from the T213L256 AGCM is already affected by the equatorial QBO in that model. While Rayleigh friction is used in MIROC-mid to decrease wind speeds in the stratosphere, it is not used in MIROC-kissme, as the friction can be represented by the Hines parameterization.

2.4 Experimental set-up

The results from MIROC-kissme and MIROC-mid are compared. Both models are run as coupled climate models in which the components for the atmosphere, ocean, sea ice, land, aerosols, and river are interactively coupled. The pre-industrial CO_2 concentration of 285 ppmv, as well as the pre-industrial concentration of the other greenhouse gases and emission data for aerosols, is used. The models are run for more than 50 years using similar initial conditions. The results for 10 consecutive years are averaged for comparison. For the stratospheric ozone concentration, MIROC-mid uses a monthly climatology in the absence of the Antarctic ozone hole, while MIROC-kissme explicitly calculates the ozone and other chemical constituents under the pre-industrial conditions, that is without any anthropogenic chlorine and the absence of an Antarctic ozone hole. Differences in the ozone concentration in the models are sufficiently small so that the conclusions in the following section are not changed if the same monthly climatology data for ozone are used in MIROC-kissme.

3. Results

Fig. 2 shows the horizontal distribution of the water vapor mixing ratio at 100 hPa during December-January-February. Results from MIROC-mid exhibit an excess of water vapor around and downstream of the mountainous regions. This is primarily caused by numerical diffusion associated with the advection of humidity across the slopes of the σ coordinate surface. The results from MIROC-kissme show a realistic distribution of the water vapor. There are two distinct minima above the maritime
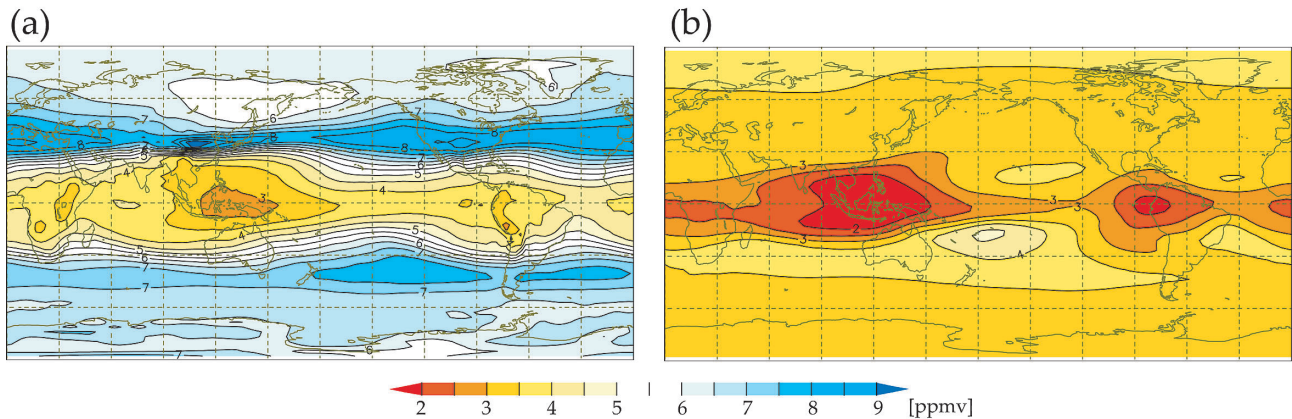
(a)

(b)

Fig. 2 December-January-February average of the water vapor mixing ratio at 100 hPa for MIROC-mid (a) and MIROC-kissme (b). The contour interval is 0.5 ppmv. Blue color shows the wet region.
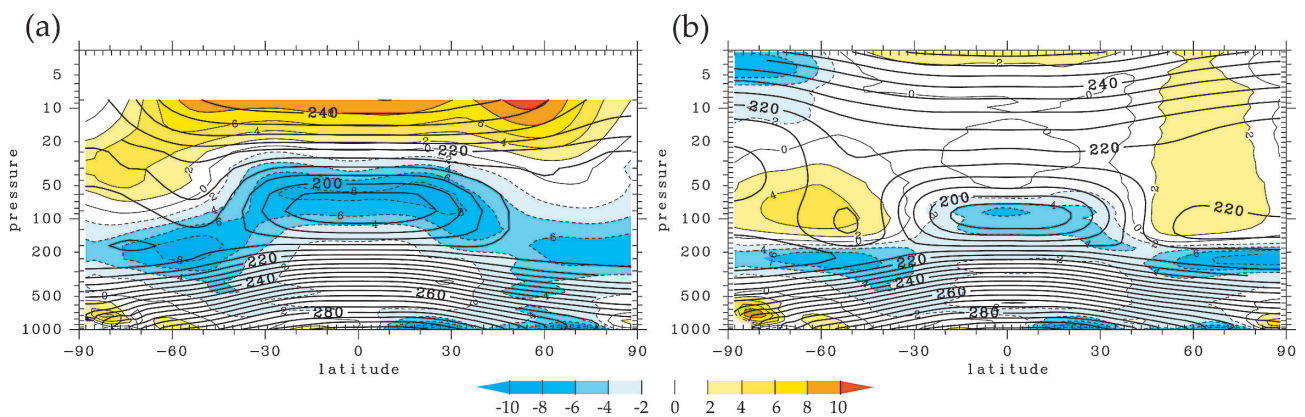
(a)

(b)

Fig. 3 Annual average of the zonal mean temperature for MIROC-mid (a) and MIROC-kissme (b). The contour interval is 10 K. Shading shows the temperature bias compared to the 1994-2001 average of the Met Office assimilation data. The contour interval is 2 K. Blue shows the cold bias.

continent and the tropics of South America, while there is a maximum over the middle Pacific in the Southern Hemisphere. This distribution is qualitatively similar to that for the ERA-40 re-analysis data [23].

Fig. 3 shows the meridional distribution of the annual average zonal mean temperature and its bias compared to the Met Office assimilation data [24], which are averaged for 1994–2001. The results from MIROC-mid have large cold biases near the tropical tropopause and in the extratropical lower stratosphere. These cold biases are dramatically decreased by the new radiative scheme. The remaining cold bias near the tropopause is probably associated with the treatment of ice clouds in the model. Alternatively, it suggests that further improvement is required in the radiative scheme.

The decrease of the cold bias in the extratropical lower stratosphere is partly due to the improvement of water vapor distribution resulting from the use of the σ-pressure hybrid coordinate system. A warm bias in the Southern Hemisphere lower stratosphere is associated with the pre-industrial condition, while the effects of the ozone hole lower the polar temperature for the present day climatology. Temperature biases near the surface are not considered. They are partly caused by issues related to properly determining the cloud distribution. This situation needs to be addressed in a separate study.

Fig. 4 shows the meridional structure of the zonal-mean zonal wind in January, over which the Met Office zonal wind is overlaid. The strength of the upper part of the subtropical jet is overestimated in results from MIROC-mid. The results from MIROC-kissme show a better correlation with the real data. This can be attributed to the decrease in the cold bias near the tropopause. The improved meridional structure of the subtropical jet may alter the vertical flux of wave activity propagating into the stratosphere through changes in the refractive index. Atmospheric waves in these models can be analyzed in future work.

Fig. 5 shows the July climatology of the gravity wave source function, which is used in the Hines gravity wave
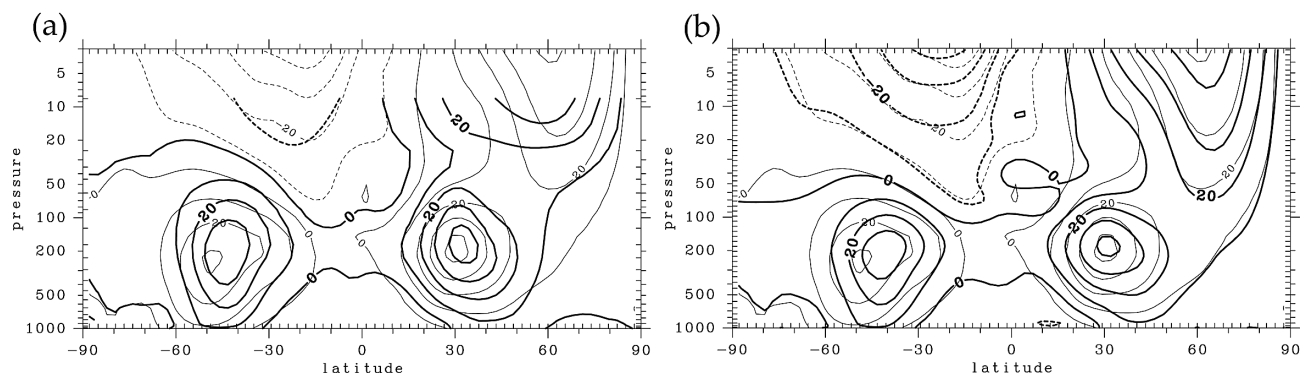
(a)

(b)

Fig. 4 December-January-February average of the zonal mean zonal wind for the MIROC-mid (a) and MIROC-kissme (b). The contour interval is 10 m·s^{-1}. Thin contours show the 1994-2001 average of the Met Office assimilation data.

√Fji and Fh for n>42 GWs at 70hPa   July

→ : 0.04 [Pa**0.5]

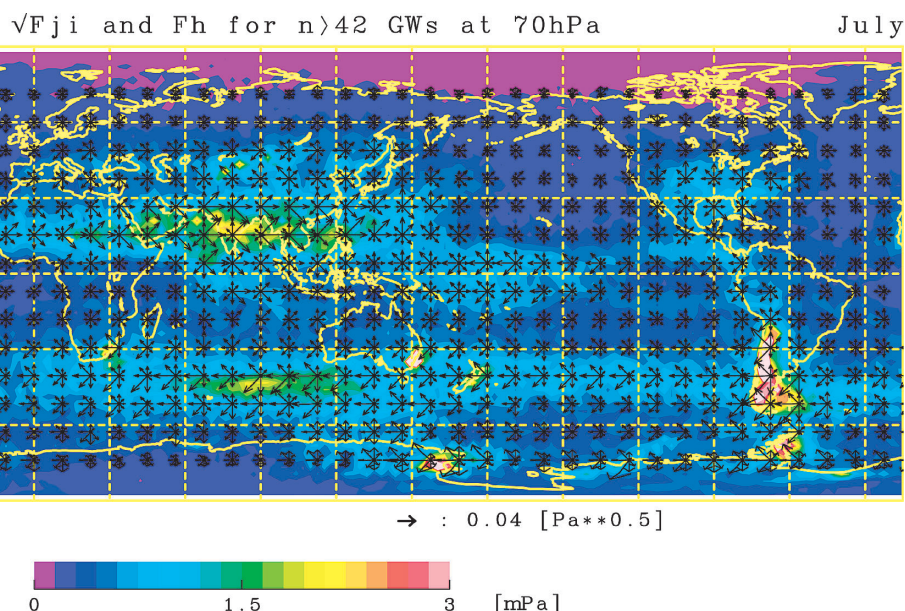0   1.5   3   [mPa]

Fig. 5 The source function used for the Hines parameterization. Arrows show the eight azimuthal components for the monthly averaged vertical flux of the horizontal momentum associated with small scale (< 950 km) gravity waves, which are derived using the result of the T213L256 AGCM. The length of the arrows shows the square root of the momentum flux for better visualization. Color shows the magnitude of the momentum flux, which is represented by the square root average of the eight azimuthal components.

drag parameterization (see Section 2.3 for a description). Non-orographic gravity waves with large momentum fluxes are mainly emitted from the cumulus convection associated with tropical cyclones, cloud clusters, and extratropical low-pressure systems. Directions of wave propagation are mostly towards the upstream of the background large-scale winds. Eastward propagating gravity waves are dominant in an easterly wind region associated with the Indian summer monsoon circulation. Westward propagating gravity waves are dominant at the Southern Hemisphere mid-latitudes, whose dissipation causes decelerations of the wintertime westerly jet in the strato-

sphere and mesosphere. The source function includes some orographic gravity wave signatures over Antarctica and the South Andes. They are difficult to separate from the non-orographic gravity waves, because they have a wave structures that varies with time [15].

Fig. 6 shows the meridional distribution of the zonal-mean zonal wind for MIROC-kissme, as well as the CIRA86 wind [25]. In January, the model accurately simulates the meridional structure of the wintertime westerly jet in the stratosphere. An axis of the westerly jet exists between 60°N and 70°N below about 1 hPa, while it exists at lower latitudes in the mesosphere. The strength
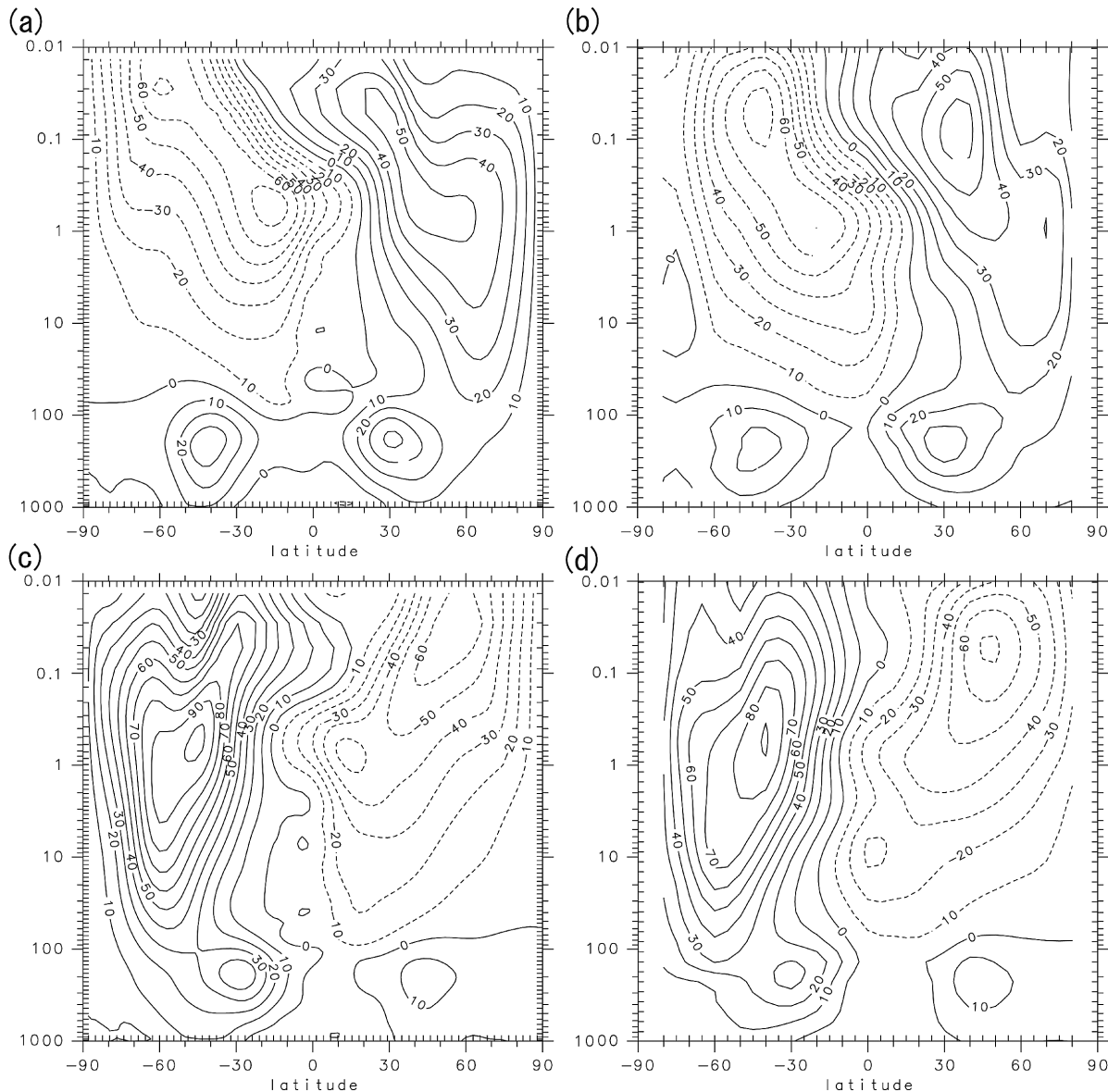
Fig. 6 The zonal mean zonal wind in January for MIROC-kissme (a) and CIRA86 (b), and in July for MIROC-kissme (c) and CIRA86 (d). The contour interval is 10 m·s^{-1}. Dashed contours show the easterly winds.

of the westerly wind is comparable to the CIRA wind in the lower stratosphere, while it is slightly overestimated in the upper stratosphere and mesosphere. In July, the modeled Southern Hemisphere westerly jet has similar characteristics to those observed. The center of the westerly jet tilts equatorward with increasing altitude above about 10 hPa. The mesospheric westerly jet has a double peak structure. The strength of the westerly wind is overestimated above the middle stratosphere by about 10–20 m·s^{-1}, which is mainly due to a lack of effects for the horizontal propagation of gravity waves in the Hines scheme [19]. The easterly jet in the summer hemisphere middle atmosphere is also reasonably simulated. The center of its maximum shifts poleward with increasing altitude from the upper stratosphere to the mesosphere. Wind speeds of

the easterly jet are also realistic. These results show that the model with Hines parameterization and the given source function reproduces reality accurately.

Fig. 7 shows the time evolution of the monthly averaged equatorial zonal mean zonal wind for MIROC-kissme. The stratopause semi-annual oscillation is seen near 1 hPa [26]. It starts in the mesosphere and propagates downward to the stratopause height. The zonal wind oscillation in the upper mesosphere has an opposite phase to that near the stratopause. These characteristics are qualitatively reasonable, although observations in the mesosphere are insufficient for quantitative comparisons. In the lower stratosphere, a QBO-like zonal wind oscillation is seen. The typical maximum wind speeds are about 13 m·s^{-1} for the westerly phase and about 27 m·s^{-1} for
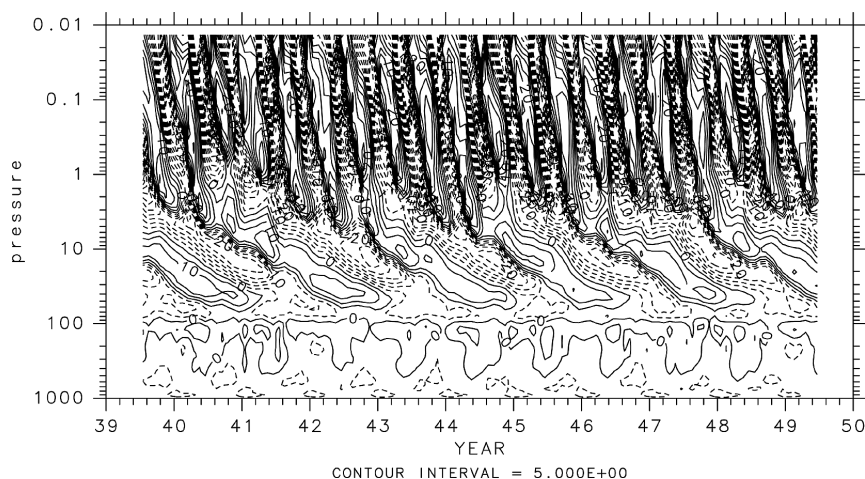
Fig. 7 Time evolution of the monthly averaged zonal mean zonal wind at the equator. The contour interval is 5 m·s⁻¹. Dashed contours show the easterly winds.

the easterly phase. The model underestimates the amplitude of the QBO by about 5 m·s⁻¹. Periods of the modeled QBO-like oscillation are about 18 months, while those observed average approximately 28 months [27]. The amplitude and period of the modeled QBO-like oscillation strongly depends on the strength of the gravity wave source used in the Hines parameterization. Careful tuning of the source function in the tropics may allow the model to reproduce a more realistic QBO-like oscillation. This tuning is beyond the scope of this study. The tuning should not be a difficult task, because other GCMs with the Hines gravity wave drag parameterization have reproduced quite realistic QBO-like oscillation [28, 29]. However, the next step is to consider the temporal evolution of the gravity wave source function associated with global warming [30, 31]. Further observations and model experiments should be required to reduce uncertainly in future changes in gravity waves and the QBO.

4. Conclusions

Compared with the MIROC-mid, the dynamical and physical processes in the stratosphere determined by MIROC-kissme are much better. The hybrid σ-pressure vertical coordinate system reduces the moisture bias. The cold biases near the tropical tropopause and in the extratropical lower stratosphere are decreased by the updated radiative scheme. The overestimation of the westerly wind in the upper part of the tropospheric subtropical jet is also decreased. This can be associated with the improvement in the thermal structure near the tropopause. The general circulation in the middle atmosphere is successfully simulated using the Hines gravity wave drag parameterization with the source function derived from the high-resolution AGCM. It is expected that a more

realistic future projection for global warming can be obtained using MIROC-kissme, which has an improved stratosphere. The realistic thermal structure around the tropopause allows an accurate evaluation of climate forcing due to greenhouse gases. The stratosphere-troposphere exchange of greenhouse gases, such as ozone, water vapor, and methane, can be calculated more accurately. Future studies will consider the effects of the QBO and solar variability on the dynamical and thermal fields, as well as on atmospheric chemistry. Distribution of the modeled chemical constituents and statistics for the transport processes in the MIROC-kissme will be studied.

Acknowledgments

(This article is reviewed by Dr. Takeshi Enomoto.)

References

[1] M. Kawamiya, C. Yoshikawa, T. Kato, H. Sato, K. Sudo, S. Watanabe, and T. Matsuno, Development of an Integrated Earth System Model on the Earth Simulator, *Journal of the Earth Simulator*, vol.**4**, pp.18–30, 2005.

[2] IGBP, Science plan and implementation strategy, *IBGP Report*, No.55, IGBP Secretariat, Stockholm, 76pp, 2006.

[3] V. Erying, N. Buchart, D. W. Waugh, H. Akiyoshi, J. Austin, S. Bekki, G. E. Bodeker, B. A. Boville, C. Brühl, M. P. Chipperfield, E. Cordero, M. Dameris, M. Deushi,

V. E. Fioletov, S. M. Frith, R. R. Garcia, A. Getteleman, M. A. Giorgetta, V. Grewe, L. Jourdain, D. E. Kinnison, E. Mancini, E. Manzini, M. Marchand, D. R. Marsh, T. Nagashima, P. A. Newman, J. E. Nielsen, S. Pawson, G. Pitari, D. A. Plummer, E. Rozanov, M. Schracer, T. G. Shepherd, K. Shibata, R. S. Stolarski, H. Struthers, W. Tian, and M. Yoshiki, Assessment of temperature, trace species, and ozone in chemistry-climate model simulations of the recent past, *J. Geophys Res.*, vol.**111**, D23308, doi:10.1029/2006JD007327, 2006.

[4] N. Buchart and A. A. Scaife, Removal of chlorofluorocar-bons by increased exchange between the stratosphere and troposphere in a changing climate, *Nature*, vol.**410**, pp.799–802, 2001.

[5] K. Sudo, M. Takahashi, and H. Akimoto, Future changes in stratosphere-troposphere exchange and their impact on future tropospheric simulations, *Geophys. Res. Lett.*, vol.**30**, 2256, doi:10.1029/2004GL020794, 2003.

[6] K. Kodera, On the origin and nature of interannual variabil-ity of the winter stratospheric circulation in the northern hemisphere, *J. Geophys. Res.*, vol.**100**, pp.14077–14087, 1995.

[7] K. Matthes, Y. Kuroda, K. Kodera, and U. Langematz, Transfer of the solar signal from the stratosphere to the troposphere: Northern winter, *J. Geophys. Res.*, vol.**111**, D06108, doi:10.1029/2005JD006283, 2006.

[8] S. Watanabe, T. Hirooka, and S. Miyahara, Interannual variations of the general circulation and polar stratospheric ozone losses in a general circulation model, *J. Meteorol. Soc. Japan*, vol.**80**, no.4b, pp.877–895, 2002.

[9] K-1 model developers, K-1 coupled model (MIROC) description, *K-1 Technical Report*, vol.**1**, H. Hasumi and S. Emori (eds.), Center for Climate System Research, University of Tokyo, 34pp., 2004.

[10] T. Nozawa, T. Nagashima, T. Ogura, T. Yokohata, N. Okada, and H. Shiogama, Climate change simulations with a coupled ocean-atmosphere GCM called the Model for Interdisciplinary Resarch on Climate: MIROC, *CGER'S SUPERCOMPUTER MONOGRAPH REPORT*, vol.**12**, Center for Global Environmental Research, National Institute for Environmental Studies, Tsukuba, Japan, 2007.

[11] M. Takahashi, Simulation of the stratospheric quasi-bien-nial oscillation using a general circulation model, *Geophys. Res. Lett.*, vol.**23**, pp.661–664, 1996.

[12] M. Takahashi, Simulation of the stratospheric quasi-bien-nial oscillation in a general circulation model, *Geophys. Res. Lett.*, vol.**26**, pp.1307–1310, 1999.

[13] S. Watanabe and M. Takahashi, Kelvin waves and ozone Kelvin waves in the quasi-biennial oscillation and semian-nual oscillation: A simulation by a high-resolution chem-istry-coupled general circulation model, *J. Geophys. Res.*,

vol.**110**, D18303, doi:10.1029/2004JD005424, 2005.

[14] H. Miura, Vertical differencing of the primitive equations in a σ-p hybrid coordinate (for spectral AGCM), *CCSR Internal Report*, pp.1–19, University of Tokyo, 2002.

[15] S. Watanabe, K. Sato, and M. Takahashi, A general circu-lation model study of orographic gravity waves over Antarctica excited by katabatic winds, *J. Geophys. Res.*, vol.**111**, D18104, doi:10.1029/2005JD006851, 2006.

[16] M. Sekiguchi and T. Nakajima, The study of the absorp-tion process and its computational optimization in an atmospheric general circulation model, J. Quant. Spectrosc. Radiat. Transfer (to be submitted).

[17] D. C. Fritts and M. J. Alexander, Gravity wave dynamics and effects in the middle atmosphere, *Rev. Geophys.*, vol.**41**, 1003, doi:10.1029/2001RG000106, 2003.

[18] N. A. McFarlane, The effect of orographically excited gravity wave drag on the general circulation of the lower stratosphere and troposphere, *J. Atmos. Sci.*, vol.**44**, pp.1775–1800, 1987.

[19] S. Watanabe, Y. Kawatani, Y. Tomikawa, K. Miyazaki, M. Takahashi, and K. Sato, General aspects of a T213L256 middle atmosphere general circulation model, *J. Geophys. Res.* (submitted).

[20] C. O. Hines, Doppler-spread parameterization of gravity-wave momentum deposition in the middle atmosphere. Part 2: Broad and quasi monochromatic spectra, and implementation, *J. Atmos. Solar Terr. Phys.*, vol.**59**, pp.387–400, 1997.

[21] D. L. Wu and J. W. Waters, Satellite observations of atmospheric variances: A possible indication of gravity waves, *Geophys. Res. Lett.*, vol.**23**, pp.3631–3634, 1996.

[22] T. Tsuda, M. Nishida, C. Rocken, and R. H. Ware, A glob-al morphology of gravity wave activity in the stratosphere revealed by the GPS occultation data (GPS/MET), *J. Geophys. Res.*, vol.**105**, pp.7257–7273, 2000.

[23] S. M. Uppala, P. W. Kållberg, A. J. Simmons, U. Andrae, V. da Costa Bechtold, M. Fiorino, J. K. Gibson, J. Haseler, A. Hernandez, G. A. Kelly, X. Li, K. Onogi, S. Saarinen, N. Sokka, R. P. Allan, E. Andersson, K. Arpe, M. A. Balmaseda, A. C. M. Beljaars, L. van de Berg, J. Bidlot, N. Bormann, S. Caires, F. Chevallier, A. Dethof, M. Dragosavac, M. Fisher, M. Fuentes, S. Hagemann, E. Holm, B. J. Hoskins, L. Isaksen, P. A. E. M. Janssen, R. Jenne, A. P. McNally, J.-F. Mahfouf, J.-J. Morcrette, N. A. Rayner, R. W. Saunders, P. Simon, A. Sterl, K. E. Trenberth, A. Untch, D. Vasiljevic, P. Viterbo, and J. Woollen, The ERA-40 re-analysis, *Quart. J. R. Meteorol. Soc.*, vol.**131**, pp.2961–3012, doi:10.1256/qj.04.176, 2005.

[24] R. Swinbank and A. O'Neill, A stratosphere-troposphere data assimilation system, *Mon. Wea. Rev.*, vol.**122**, pp.686–702, 1994.

[25] D. Rees, J. J. Barnett, and K. Labitzke (ed.), CIRA 1986,

Part II Middle Atmosphere Models, *Advances in Space Research (COSPAR)*, vol.**10**, no.12, 1990.

[26] I. Hirota, Equatorial waves in the upper stratosphere and mesosphere in relation to the semiannual oscillation of the zonal wind, *J. Atmos. Sci*., vol.**35**, pp.714–722, 1978.

[27] M. P. Baldwin, L. J. Gray, T. J. Dunkerton, K. Hamilton, P. H. Haynes, W. J. Randel, J. R. Holton, M. J. Alexander, I. Hirota, T. Horinouchi, D. B. A. Jones, J. S. Kinnersley, C. Marquardt, K. Sato, and M. Takahashi, The Quasi-Biennial Oscillation, *Rev. of Geophys.*, vol.**39**, pp.179–229, 2001.

[28] M. A. Giorgetta, E. Manzini, and E. Roeckner, Forcing of the quasi-biennial oscillation from a broad spectrum of atmospheric waves, *Geophys. Res. Lett.*, vol.**29**, no.8, pp.86–1 – 86–4, 2002.

[29] A. A. Scaife, N. Butchart, C. Warner, D. Stainforth, W. Norton, and J. Austin, Realistic quasi-biennial oscillations in a simulation of the global climate, *Geophys. Res. Lett.*, vol.**27**, pp.3481–3484, 2000.

[30] S. Watanabe, T. Nagashima, and S. Emori, Impact of global warming on gravity wave momentum flux in the lower stratosphere, *SOLA*, vol.**1**, pp.189–192, 2005.

[31] M. A. Giorgetta and M. C. Doege, Sensitivity of the quasi-biennial oscillation to CO_2 doubling, *Geophys. Res. Lett*., vol.**32**, L08701, doi:10.1029/2004GL021971, 2005.